Composite Structures 99 (2013) 181–192

Contents lists available at SciVerse ScienceDirect

Composite Structures

journal homepage: www.elsevier.com/locate/compstruct

Robust design optimisation of advance hybrid (fiber–metal) composite structures ☆

DongSeop Lee [a,c], Carlos Morillo [b,*], Sergio Oller [a,b], Gabriel Bugeda [a,b], Eugenio Oñate [a,b]

[a] Centre Internacional de Metodes Numerics en Enginyeria (CIMNE), Edificio C1, Gran Capitan, s/n, 08034 Barcelona, Spain
[b] Universitat Politecnica de Catalunya, Barcelona Tech (UPC), Edificio C1, Gran Capitan, s/n, 08034 Barcelona, Spain
[c] Deloitte Analytics, Deloitte Consulting LLC, Seoul, Republic of Korea

ARTICLE INFO

Article history:
Available online 20 December 2012

Keywords:
Stacking sequence
Hybrid (fiber–metal) composite structures
Multi-Objective Optimisation
robust design optimisation
Finite Element Analysis

ABSTRACT

Hybrid Composite Structures (HCSs) are consisting of alternating layers of Fiber-Reinforced Polymer and metal sheets. Mechanical properties and responses for off-design conditions of HCSs can be improved using an innovative methodology coupling Multi-Objective Genetic Algorithm and robust design method. The concept of robust design approach ensures that a structure will be tolerant to unexpected loading and operating conditions. In this paper, two applications are considered; the first is to maximise the stiffness of the HCS while minimising its total weight through a Multi-Objective Design Optimisation. The second application considers a Robust Multi-Objective Design Optimisation (RMDO) to minimise total weight of HCS and to minimise both, the normalised mean displacement and the standard deviations of displacement, considering critical load cases. For the optimisation process, a distributed/parallel Multi-Objective Genetic Algorithm in robust multi-objective optimisation platform is used and it is coupled to a Finite Element Analysis based composite structure analysis tool to find the optimal combination of laminates sequences for HCSs. Numerical results show the advantages in mechanical properties of HCS over the metal structures, and also the use of RMDO methodology to obtain higher characteristics of HCS in terms of mechanical properties and its stability at the variability of load cases.

1. Introduction

The development of hybrid composites has been motivated from aerospace and marine industries to improve mechanical properties and lower operating cost [1]. The definition of Hybrid Composite Structures (HCSs) is consisted of several thin metal alloy sheets and plies of continuous Fiber-Reinforced Polymer (FRP) materials. HCSs have both the advantages of metallic and composite materials, including good plasticity, impact resistance, processability, low weight and excellent fatigue properties. They were originally developed at Delft University of Technology at the beginning of 1980 [2]. Recently, some new hybrid materials have been developed like the newest metal laminates consisting of thin titanium plies sandwiched by layers of polymer matrix composites. Boeing Airplane Company refers to this class of materials as Ti–Gr (titanium–graphite), while others have referred to them as Hybrid Titanium Composite Laminates (HTCLs) [3]. In HCS, the metal protects the FRP core from environmental effects such as thermal degradation and moisture ingress while potentially providing higher impact resistance and bearing properties. The FRP core has higher stiffness-to-weight ratios than monolithic metal that is less sensitive to fatigue effects. In addition, the composite can potentially outperform either of two constituent materials in elevated temperature structural applications [4].

From HCS literature reviews, it can be seen that most of researchers focused on experimental test of mechanical properties [3–12], and few studies deal with the optimisation of these hybrid composites; Nam et al. [13] consider a single-objective optimisation of HCS using GA to maximise the composite strength by altering the ply orientation of the composite. Peng et al. [14] consider

Abbreviations: Al-A, Aluminium 2024-T3; CAD, Computer Aided Design; CDF, Cumulative Distribution Function; CFD, Computation Fluid Dynamic; FEA, Finite Element Analysis; FEM, Finite Element Method; FRP, Fiber-Reinforced Polymer; GA, Genetic Algorithm; HCSs, Hybrid Composite Structures; HTCL, Hybrid Titanium Composite Laminate; Mo, Metal Orientation; MODO, Multi-Objective Design Optimisation; MOGA, Multi-Objective Genetic Algorithm; MS, metal structure; MS Al-A, reference Aluminium 2024-T3 metal structure; MS Ni-A, reference Nickel Aluminium Bronze UNS C63000 metal structure; MS Ti-A, reference Titanium Grade 12 Annealed metal structure; Mt, Metal thickness; Ni-A, Nickel Aluminium Bronze UNS C63000; NMD, normalised mean displacement; PDF, Probability Density Function; PM, Pareto member; PSO, Particle Swarm Optimisation; RDO, robust design optimisation; RMDO, Robust Multi-Objective Design Optimisation; RMOGA, Robust Multi-Objective Genetic Algorithm; RMOP, Robust Multi-objective Optimisation Platform; SDD, Standard Deviations of the Displacement; Ti-A, Titanium Grade 12 Annealed; Ti–Gr, Titanium–Graphite.

☆ http://www.cimne.com.

* Corresponding author.
E-mail addresses: dslee@cimne.upc.edu (D. Lee), cmorillo@cimne.upc.edu (C. Morillo), sergio.oller@upc.edu (S. Oller), bugeda@cimne.upc.edu (G. Bugeda), onate@cimne.upc.edu (E. Oñate).

0263-8223/$ - see front matter © 2012 Elsevier Ltd. All rights reserved.
http://dx.doi.org/10.1016/j.compstruct.2012.11.033

optimal strength design for FRP and HCS using Particle Swarm Optimisation (PSO) to minimise the failure by optimising fiber orientation angles. However, in practical situations, it is desirable to find a structural design that optimises various performances simultaneously at off-design conditions. Although the need for considering the multiple structural behaviours simultaneously as a set of objective functions is thus apparent, these previous studies are limited to the case of a single objective function.

Robust design optimisation (RDO) proposed by Taguchi [15] can be an emerging design method in composite structures where principal objective is to improve product quality by controlling the uncertainty effect. In engineering, the RDO cannot be ignored since the variations of manufacturing process parameters, environmental aspect and loads life conditions can affect the solution quality in terms of mean performance and its sensitivity [16,17]. Some researchers have considered such variances or tolerances applying uncertain design conditions in fiber laminated composites. Walter and Hamilton [18] described a procedure to design laminated plates for a maximisation of bucking load with manufacturing uncertainty in the ply orientation angle. Adali et al. [19] present an optimal design of composite laminates subjected to biaxial compressive loads belonging to a given uncertainty domain under the worst possible case of biaxial compressive loading. Liao and Chiou [20] proposed a method based on anti-optimisation technique by adding extra sensitivity terms in design constraints that is used for the robust optimum design of fiber reinforced composites with manufacturing uncertainties. Antonio and Hoffbauer [21] develop a mixed formulation of reliability-based design optimisation and robust design optimisation for reinforced composites, considering the ply angle, load factor, the elastic and strength materials properties as design variables. Lee et al. [22] set the differences between the damage tolerant design and robust design analysing composite panels. They studied the effect of laminate stacking sequence on the robustness and present a methodology to quantify it using Finite Element Analysis. Literature reviews considering the concept of robust design optimisation in composite structures show that only manufacturing uncertainties have been considered whereas uncertainties in loading conditions have not.

In this paper, a robust multi-objective optimisation methodology is developed for a hybrid (fiber–metal) composite structure (HCS) design considering a set of uncertain critical load cases (bending, shear and torsion) and also treating manufacturing process parameters as design variables. The paper investigates the robust multi-objective stacking sequence design optimisation for HCSs using a distributed/parallel Genetic Algorithm (GA) in Robust Multi-objective Optimisation Platform (RMOP) developed at CIMNE coupled with a Finite Element Analysis (FEA) based composite structure analysis tool named Compack [23–25]. Two HCS applications are addressed; the first application in a multi-objective manner is to improve mechanical properties (both weight and stiffness) of HCS, which is modelled as a simply (two opposite sides) supported quadrangular plate. The second application considers a robust design optimisation of HCS that is formulated to minimise its total weight while maximising HCS stiffness quality in terms of mean and standard deviation of displacement. In the second application, the boundary condition is set as one side rigid rectangular hybrid composite plate. For HCS manufacturing design variables, 32 design parameters are considered in total: six types of fiber (aramid, glass, boron, and carbon fibers), eleven fiber thicknesses, twelve fiber orientation angles, and also three different high performed metals allows (Aluminium 2024-T3 (Al-A), Titanium Grade 12 Annealed (Ti-A) and Nickel Aluminium Bronze UNS C63000 (Ni-A)).

The rest of this paper is organised as follows; Section 2 describes a methodology for HCS design optimisation. Section 3 presents a composite structure analysis tool. Section 4 considers two real-world HCS design optimisations. Section 5 concludes overall numerical results and present future research avenues.

2. Methodology

2.1. Multi-Objective Design Optimisation

Often, engineering design problems require a simultaneous optimisation of conflicting objectives and an associated number of constraints. Unlike single objective optimisation problems, the solution is a set of points known as Pareto optimal set. Solutions are compared to other solutions using the concept of Pareto dominance. A multi-criteria optimisation problem can be formulated as

Maximise/minimise the functions:

$$f_i(x)_i \quad i = 1, \ldots, N \tag{1}$$

Subject to constraints:

$$\begin{aligned} g_j(x) &= 0 \quad j = 1, \ldots, M \\ h_k(x) &\le 0 \quad k = 1, \ldots, M \end{aligned} \tag{2}$$

where f_i, g_j, h_k are, respectively, the objective functions, the equality and the inequality constraints. N is the number of objective functions and x is an n – dimensional vector where its arguments are the decision variables. For a minimisation problem, a vector x_1 is said partially less than vector x_2 if:

$$\forall_i f_i(x_1) \le f_i(x_2) \quad \text{and} \quad \exists_i f_i(x_1) < f_i(x_2) \tag{3}$$

In this case the solution x_1 dominates the solution x_2.

As Genetic Algorithms (GAs) evaluate multiple populations of points, they are capable of finding a number of solutions in a Pareto set. Pareto selection ranks the population and selects the non-dominated individuals for the Pareto fronts. A Genetic Algorithm that has capabilities for multi-objective optimisation is termed Multi-Objective Genetic Algorithms (MOGAs). Theory and applications of MOGAs can be found in Refs. [26–28].

2.2. Robust design optimisation

A robust design method, also called the Taguchi Method (uncertainty), pioneered by Taguchi [15], improves the quality of engineering productivity. An optimisation problem can be define as

Maximization/minimization:

$$f = f(y_1, \ldots, y_n, y_{n+1}, \ldots, Y_m) \tag{4}$$

where $y_1, \ldots, y_n$ represent design parameters and $y_{n+1}, \ldots, y_m$ represent uncertainty parameters. The range of uncertainty design parameters can be defined by using two statistical functions; mean (μx) and variance ($\delta x = (\sigma x)^2$) as part of the Probability Density Function (PDF). The Taguchi optimization method minimises the variability of the performance under uncertain operating conditions. Therefore in order to perform an optimisation with uncertainties, the fitness function(s) should be associated with two statistical formulas: the mean value μf and its variance δf or standard deviation $\sigma f = \sqrt{\delta f}$.

$$\mu f = \frac{1}{K}\sum_{i=1}^{k} f_i \tag{5}$$

$$\delta f = \frac{1}{K-1}\left(\sum_{i=1}^{K}(f_i - \mu f)^2\right) \tag{6}$$

where K denotes the number of subintervals of variation conditions.

The values obtained by the mean (μf) and the variance (δf) or standard deviation (σf) represent the reliability of model in terms of the magnitude of performance and stability/sensitivity at a set of uncertain design conditions.

2.3. Robust Multi-objective Optimisation Platform

RMOP is a computational intelligence framework which is a collection of population based algorithms including Multi-Objective Genetic Algorithm (MOGA) and Particle Swarm Optimisation (PSO) [26,28,29]. RMOP is easily coupled to any analysis tools such as Computation Fluid Dynamic (CFD), Finite Element Analysis (FEA) and/or Computer Aided Design (CAD) systems. In addition, it is capable to solve any engineering design applications. In this paper, a GA searching method in RMOP is used (denoted as RMOGA) under the parallel/distributed optimisation system. RMOGA uses a Pareto tournament selection operator which ensures that the new individual is not dominated by any other solutions in the tournament. Fig. 1 shows the overall algorithm for robust design optimisation problems using RMOGA.

3. Composite structure analysis tools

Compack is an analysis kit designed by Quantech and CIMNE able to use the necessary tools for the generation of a finite element model to perform structural simulations of composite material structures (see references [30–32]). Compack is able to determine the structural properties such as elastic behaviour, ultimate tensile, compression strength, and damage level of a composite material. One of the principal benefits of Compack is the capability of working with the constitutive model of the composite material in detail. To do so, it takes into account all mechanical and physical properties, amount and orientation of each of its forming fibre and matrix materials, and follows a FEM procedure to solve the structural problem.

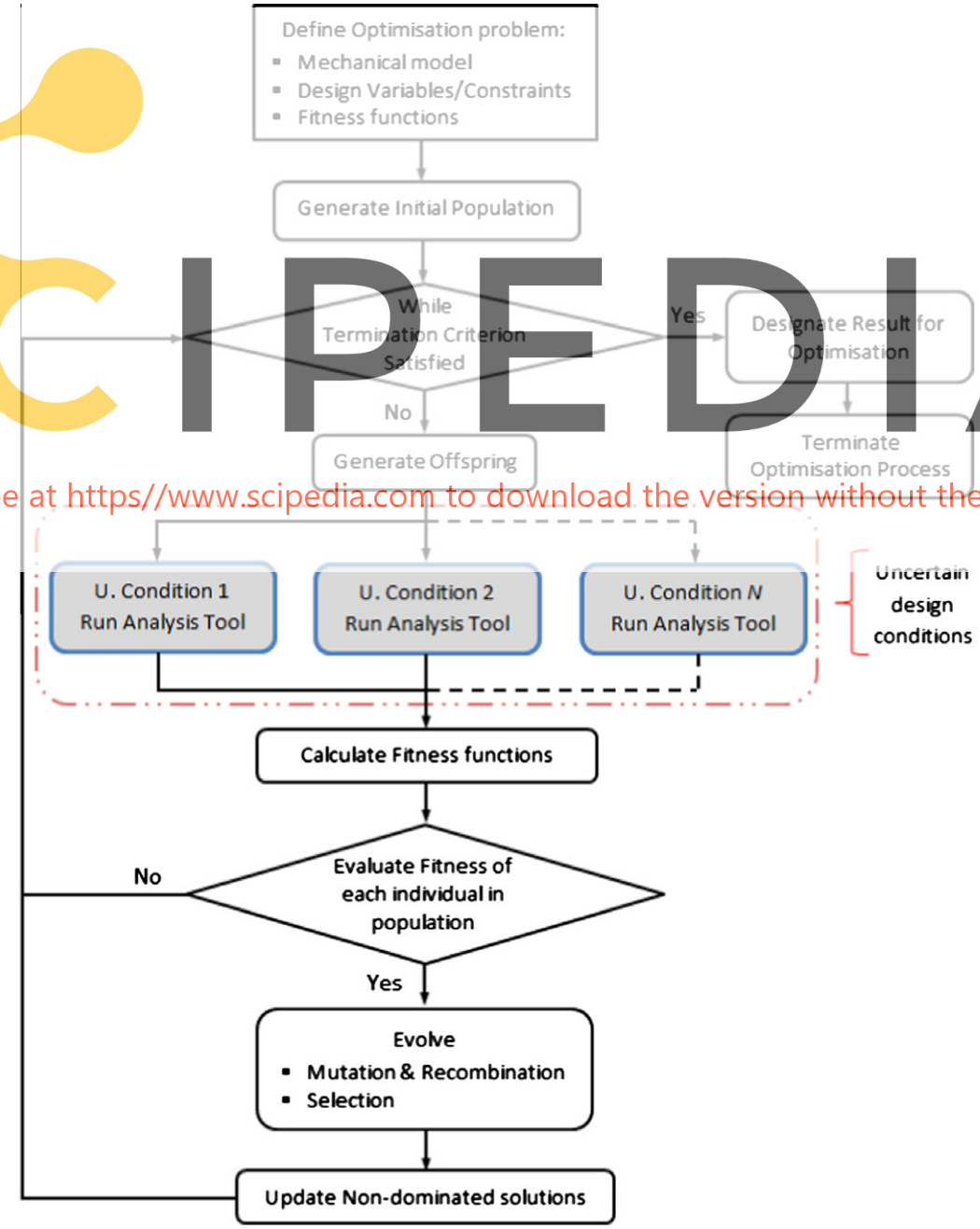

Fig. 1. Overall algorithm for robust design optimisation problems using RMOGA.

4. Advance hybrid (fiber–metal) composite structure design optimisation

This section considers two applications of advanced hybrid (fiber–metal) composite structure (HCS) using RMOGA coupled to Compack; the first problem considers a Multi-Objective Design Optimisation (MODO) design of HCS. The second problem is a Robust Multi-Objective Design Optimisation (RMDO) of HCS considering three different critical load conditions (bending, shear and torsion). Numerical results compare mechanical properties and mechanical behaviours of optimal HSCs, and three metal structures composed with Aluminium 2024-T3 (denoted as MS Al-A), Titanium Grade 12 Annealed (denoted as MS Ti-A) and Nickel Aluminium Bronze UNS C63000 (denoted as MS Ni-A).

4.1. Multi-Objective Design Optimisation of Hybrid Composite Structure

4.1.1. Problem definition

The problem treats the Multi-Objective Design Optimisation of HCSs. Fig. 2 shows the baseline of sandwich composite to optimise which has seven layers; three metals layers (top, middle and bottom) and four intermediate Fiber-Reinforced Polymer (FRP) layers; each reinforced composite layer contains 60% of fibre and 40% epoxy matrix (3501-6 Epoxy). The boundary conditions and mesh for the structural model are shown in Fig. 3 where a quadrilateral plate is simply supported in two of its sides and a constant punctual force is applied in the central position.

The objectives are formulated to minimise the total weight (W_{HCS}) while minimising the displacement (ΔD_{HCS}) of HCS as shown in Eqs. (7) and (8).

$$f_1 = \min(W_{HCS}) \tag{7}$$

$$f_2 = \min(\Delta D_{HCS}) \tag{8}$$

where ΔD_{HCS} is the total displacement for HCS composite structure.

4.1.2. Design variables

Design variables are limited to three different metals with constant thickness (0.3 mm), six fiber types, twelve orientation angles, and eleven thicknesses for the FRP layers, as shown in Tables 1–4. The details of material properties can be found in Refs. [33–35].

Fig. 4 illustrates an example for HCS configuration in this paper where it consists of four layers of FRP; Boron (layer 2), Carbon Pitch (layer 3), Carbon Rayon (layer 5) and Carbon Rayon (layer 6), thickness of 1.8 mm, 1.8 mm, 1.2 mm and 1.6 mm, and orientation angles of 45°, 15°, 15° and 45°. Additionally this hybrid composite has three metal layers of Ti-A (layer 1), Al-A (layer 4) and Al-A (layer 7). The thickness of metal layer is fixed as 0.3 mm, and the orientation angle is not considered for the metals layers.

4.1.3. Numerical results

The optimisation has run 20 h of computer time (2040 function evaluations) using ten CPUs in Dell PowerEdge 6850 (Intel(R) Xeon(TM) CPU 16 × 3.20 GHz and 32 GB RAM) machine. Fig. 5 compares Pareto optimal solutions, and three metals structures with 2 mm total thickness i.e. 4 layers with 0.5 mm thickness of Al-A, Ti-A, and Ni-A. Numerical results show that all Pareto optimal solutions have superiority in weight and stiffness as shown in Fig. 5. The proposed method offers a set of choices to the aero-structural or marine design engineer to have alternative hybrid composites instead of using metals. For instance, Pareto members 1 and 2 in Zone-A can be used instead of metal structure (MS) Al-A, Pareto members 1–5 in Zone-B can be used instead of MS Ti-A, and Pareto members 1–19 in Zone-C can be used instead of MS Ni-A.

Table 5 compares fitness values obtained by three metal structures and Pareto members 1, 4 and 19. It can be seen that Pareto members have superiority on mechanical properties; lower displacement (higher stiffness) with lower weight when compared to Al-A, Ti-A and Ni-A metal structures. More specifically, Pareto member 1 reduces the total weight by 36.5% and displacement by 45.5% when compared to Al-A structure. Pareto member 4 has the total weight reductions by 6.3% and displacement by 39.5% when compared to Ti-A, and Pareto member 19 has 2% and 75.8% weight and displacement improvement when compared with the MS Ni-A.

Table 6 presents the stacking design sequence for Pareto members 1, 4 and 19. Fig. 6 compares the displacement contours obtained for the Ti-A structure and for Pareto member 4. Numerical study on hybrid composite design clearly shows the potential of using RMOP coupled with Compack to find high strength HCS with lower weight.

4.2. Robust design optimisation of fiber metal laminated composite structures

4.2.1. Problem definition

The problem considers a robust weight optimisation of the laminate structure as shown in Fig. 7. Three uncertainty critical load cases including bending, shear and torsion are considered to increase the mechanical quality of Hybrid Composite Structure (HCS) as shown Fig. 8. The main purpose of this test case is to reinforce a metal structure with fiber composite materials by optimising type of fiber, orientation angle, thickness, and stacking sequence.

The objectives are to minimise the total weight (W_{HCS}), normalised mean displacement ($\mu\Delta D_{N\ HCS}$ denoted NMD), and the standard deviation of the displacement ($\sigma\Delta D_{A\ HCS}$ denoted SDD) of HCS composite structures as shown in Eqs. (9)–(11) respectively. The second fitness function is normalised mean displacement of reference metals structures with three layers of 0.5 mm thickness

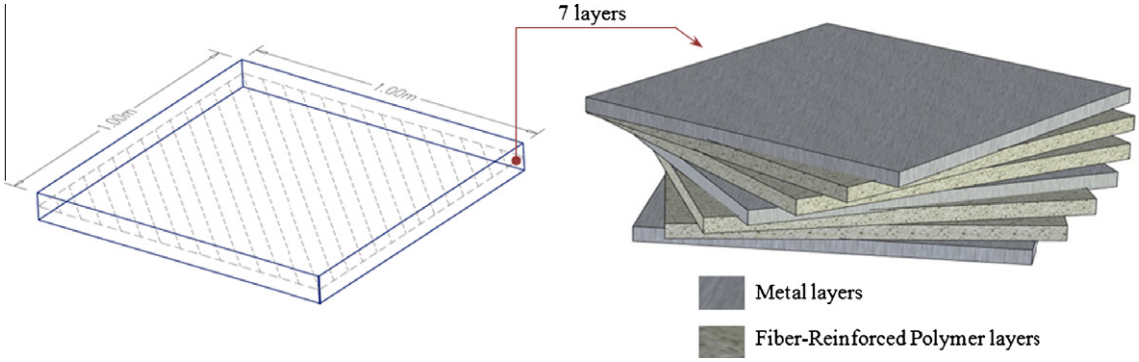

Fig. 2. Baseline fiber metal laminated composite design.

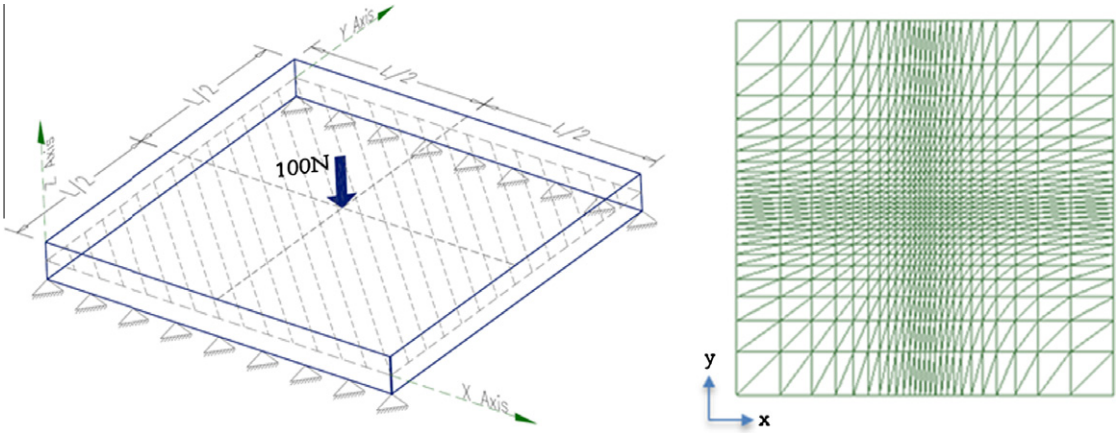

Fig. 3. Boundary conditions (left) and mesh (right) for fiber metal composite plate.

Table 1
Mechanical properties of metals and ID number.

ID #	1	2	3
Metal Name	Aluminum 2024-T3 (Al-A)	Titanium Grade 12 Annealed (Ti-A)	Nickel Aluminum Bronze UNS C63000 (Ni-A)
Density (g/cm^3)	2.78	4.5	7.58
Tensile modulus (Gpa)	73.1	103.0	115.0

Table 2
Mechanical properties of generic fibre material types and ID number.

ID #	1	2	3	4	5	6
Fiber name	Carbon pan	Carbon pich	Carbon rayon	Glass	Aramid	Boron
Density (g/cm^3)	1.825	2.025	1.6	2.55	1.44	2.45
Tensile modulus (Gpa)	276	465	41	78	138	400

Table 3
Layer thicknesses and ID number.

ID#	1	2	3	4	5	6	7	8	9	10	11
Thickness(m)	1×10^{-4}	2×10^{-4}	4×10^{-4}	6×10^{-4}	8×10^{-4}	1×10^{-3}	1.2×10^{-3}	1.4×10^{-3}	1.6×10^{-3}	1.8×10^{-3}	2×10^{-3}

Table 4
Fibre orientation angles and ID number.

ID#	1	2	3	4	5	6	7	8	9	10	11	12
Angle	0°	15°	30°	45°	60°	75°	90°	−15°	−30°	−45°	−60°	−75°

$$HCS_{config} = \begin{bmatrix} Stacking\ Sequence\ (ID) \\ Layer\ Thickness\ (ID) \\ Orientation\ Angle\ (ID) \end{bmatrix} = \begin{bmatrix} 2 & 6\ 2 & 1 & 3\ 2 & 1 \\ Mt & 10\ 10 & Mt & 7\ 9 & Mt \\ Mo & 4\ 2 & Mo & 2\ 4 & Mo \end{bmatrix}$$

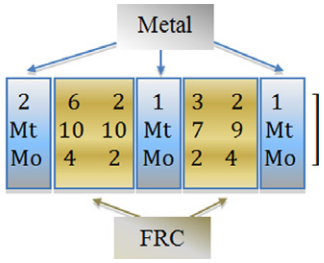

Fig. 4. Optimiser configuration for fiber metal laminated composite. (*Note*: *Mt* represents the metal thickness and *Mo* fiber orientation angle that not apply for metal layers).

(1.5 mm in total thickness) instead of using actual mean displacement. The reason is to make sure that there is an equal portion of displacement reduction for load Cases 1–3 during the optimisation process.

$$f_1 = \min(W_{HCS}) \tag{9}$$

$$f_2 = \min(\mu\Delta D_{N\_HCS}) \tag{10}$$

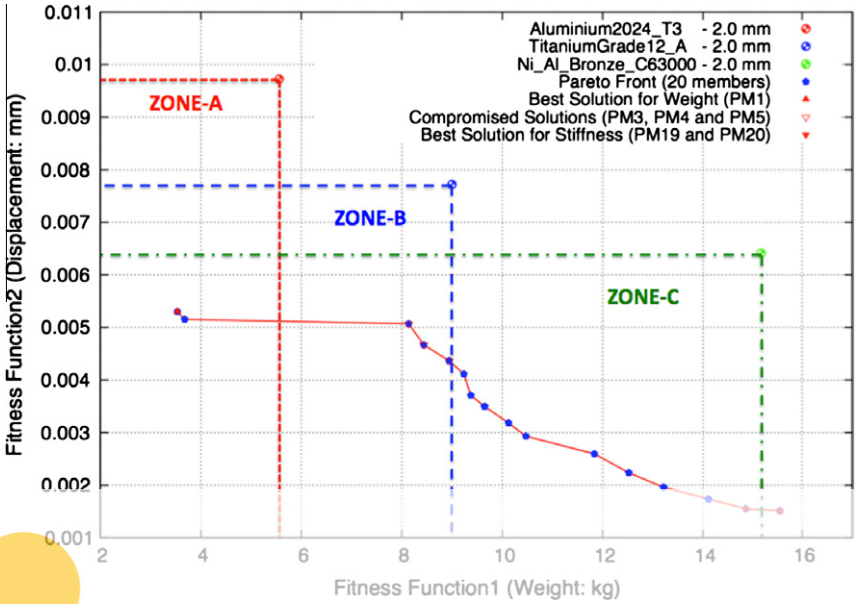

Fig. 5. Pareto optimal front for multi-objective HCS design optimisation.

Table 5
Comparison of weight and displacement obtained by three metal structures (MS) with Al-A, Ti-A and Ni-A, and Pareto members 1, 4 and 19.

MS/HCS Pareto members (PM)	Weight (kg)	Displacement (m)
MS Al-A	5.56	0.00973
Pareto member 1 (Best solution for Weight)	3.53 (−36.5%)	0.00530 (−45.5%)
MS Ti-A	9.0	0.00772
Pareto member 4 (Compromised solution)	8.43 (−6.3%)	0.00467 (−39.5%)
MS Ni-A	15.16	0.00641
Pareto member 19 (Best solution for Stiffness)	14.85 (−2.0%)	0.00155 (−75.8%)

Table 6
Stacking sequence of Pareto members 1, 4 and 19 (*Note*: *Mt* and *Mo* represent metal thickness and orientation i.e. *Mt* = 0.3 mm and *Mo* not apply for metal layers).

Pareto member	Stacking sequence (ID)	Thickness (ID)	Orientation angle (ID)
Pareto member 1 (Best Weight solution)	1131311	*Mt*11*Mt*11*Mt*	*Mo*115*Mo*11*Mo*
Pareto member 4 (Compromised Solution)	1551221	*Mt*910*Mt*13*Mt*	*Mo*32*Mo*44*Mo*
Pareto member 19 (Best stiffness solution)	2621321	*Mt*1010*Mt*79*Mt*	*Mo*42*Mo*24*Mo*

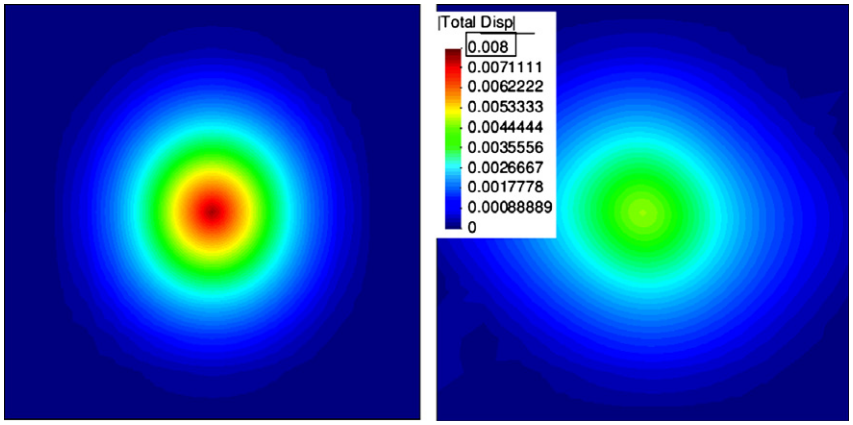

Fig. 6. Comparison of displacement contours obtained by MS Ti-AL (left) and Pareto member 4 (right) at displacement range of [0:0.008 m].

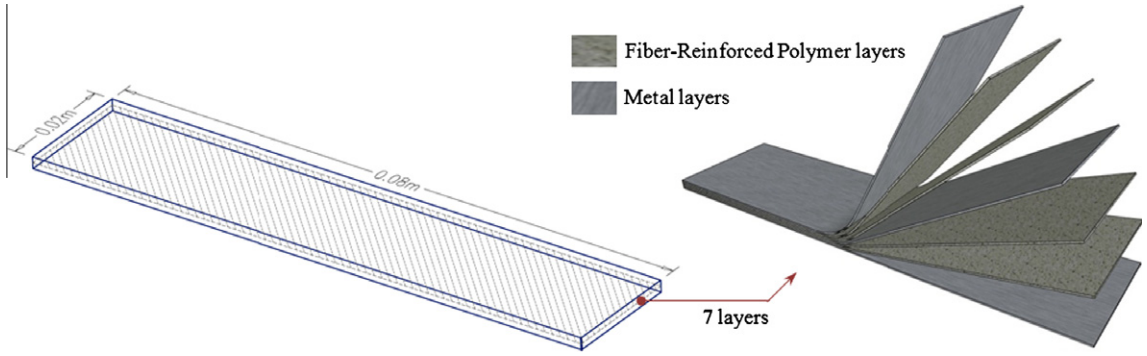

Fig. 7. Advance fiber metal laminated configuration.

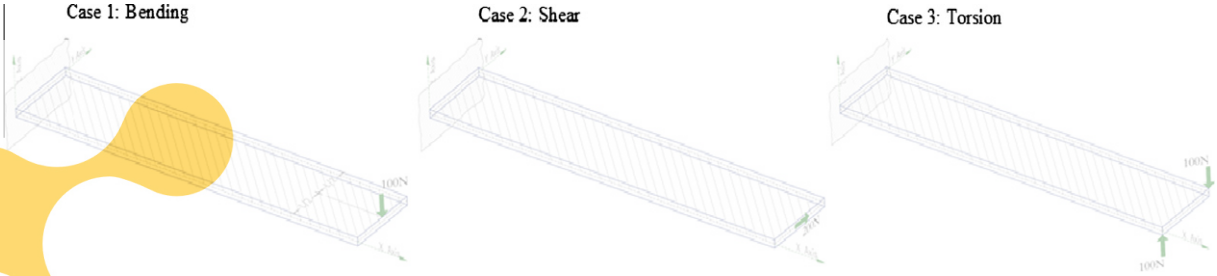

Fig. 8. Three critical uncertainty cases including bending, shear, and torsion load cases.

$$f_3 = \min(\sigma\Delta D_{A\_HCS}) \tag{11}$$

The normalised mean displacement ($\mu\Delta D_{N\_HCS}$) is determined as shown in Eq. (12);

$$\mu\Delta D_{N\_HCL}\ (\%) = \frac{100}{N_{Case}} \sum_{i=1}^{N_{Case}} \left(\frac{\Delta D_{HCSi}}{\mu\Delta D_{MSi}} \right) \tag{12}$$

where ΔD_{HCSi} is the ith case actual displacement and $\mu\Delta D_{MSi}$ is the average value of the ith case of metal structure; 1st Al-A, 2nd Ti-A and 3rd Ni-A, shown in Table 7. The standard deviation of actual displacement is

$$\sigma\Delta D_{A\_HCS} = \frac{1}{N_{Case^{-1}}} \sigma\Delta D_{A\_HCS} = \sqrt{\frac{1}{N_{Case^{-1}}} \sum_{i=1}^{N_{Case}} (\Delta D_{HCSi} - \mu\Delta D_{HCS})^2} \tag{13}$$

where

$$\mu\Delta D_{HCS} = \frac{1}{N_{Case}} \sum_{i=1}^{N_{Case}} (\Delta D_{HCSi}) \tag{14}$$

4.2.2. Design variables

The design variables for this problem are the same as considered in the Multi-Objective Design Optimisation of HCS composite structures in Section 4.1. Three types of metal: Aluminium 2024-T3 (Al-A), Titanium Grade 12 Annealed (Ti-A), Nickel Aluminium Bronze UNS C63000 (Ni-A) are considered with a constant thickness (0.3 mm), and six fiber types, twelve orientation angles, and eleven thicknesses for the FRP layers. The design variables with respective ID are presented in Tables 1–4.

4.2.3. Numerical results

The optimisation process for robust HCS composite structures design has stopped after fifty hours (680 function evaluations) using ten CPUs in Dell PowerEdge 6850 (Intel(R) Xeon(TM) CPU 16 × 3.20 GHz and 32 GB RAM) machine. Figs. 9–11 compare the Pareto optimal front obtained by the robust design optimisation and three metal structures composed by Al-A, Ti-A and Ni-A with a total thickness of 1.5 mm (3 layer of 0.5 mm). It can be seen that Pareto optimal solutions can be divided in three categories; Zone-A, Zone-B and Zone-C for the usage of Al-A, Ti-A and Ni-A respectively. Fig. 9 (weight vs. Normalized Mean Displacement (NMD)) shows that Pareto members 1 and 2 in Zone-A have lower weight and NMD than the metal structure with Al-A. In the same manner, Pareto members 2–8 in Zone-B and Pareto members 2–12 in Zone-C have lower weight and lower NMD when compared to the metal structures with Ti-A and with Ni-A respectively.

Fig. 10 (weight vs. Standard Deviation of Displacement (SDD)) shows that Pareto members 1 and 2 in Zone-A have lower weight and NMD than the metal structure with Al-A. In the same manner, Pareto members 1–8 in Zone-B and all Pareto members 1–12 in Zone-C have lower weight and lower SDD when compared to the metal structures with Ti-A and with Ni-A respectively. The details from Figs. 9 and 10 reflect that Pareto optimal solutions have lower weight and lower mean displacement with lower sensitivity at all three critical load cases when compared to the three metal structures with Al-A, Ti-A and Ni-A.

Fig. 11 illustrates NMD vs. SDD obtained by Pareto optimal front and three metal structures. It is noticed that there is a lineal increase tendency for the SDD which the increments of NMD. All

Table 7
Mean ($\mu\Delta D_{MS}\mu\Delta D_{MS}$) and standard deviation ($\sigma\Delta D_{MS}$) of displacements for three metal structures; Al-A, Ti-A and Ni-A.

	Case 1 (m)	Case 2 (m)	Case 3 (m)	$\sigma\Delta D_{MS}$ (m)
MS Al-A	0.036303	0.000505	0.002567	0.020099
MS Ti-A	0.031680	0.000363	0.001775	0.017687
MS Ni-A	0.032046	0.000321	0.001717	0.017927
$\mu\Delta D_{MS}$	0.033343	0.000396	0.002019	

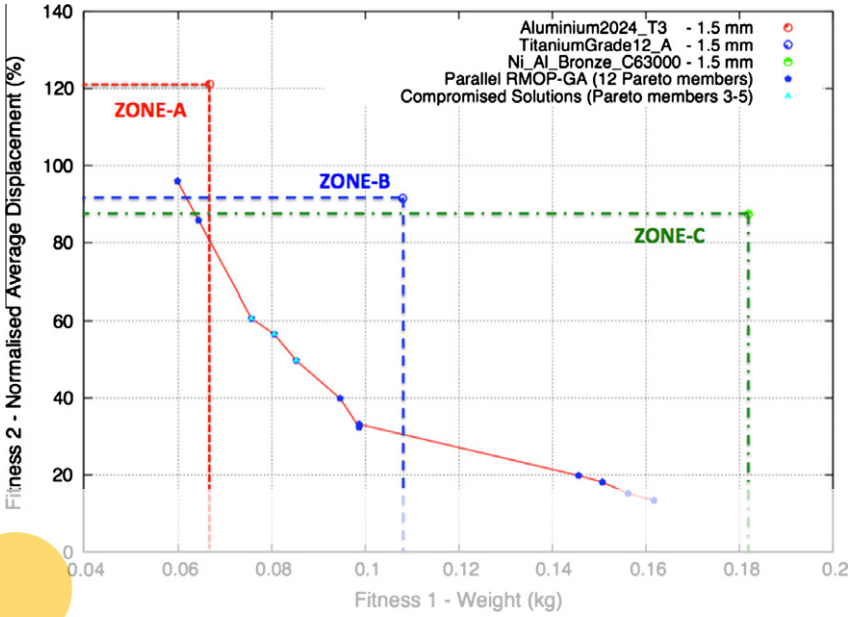

Fig. 9. Fitness 1 (Weight) vs. Fitness 2 (Normalised Mean/Average Displacement).

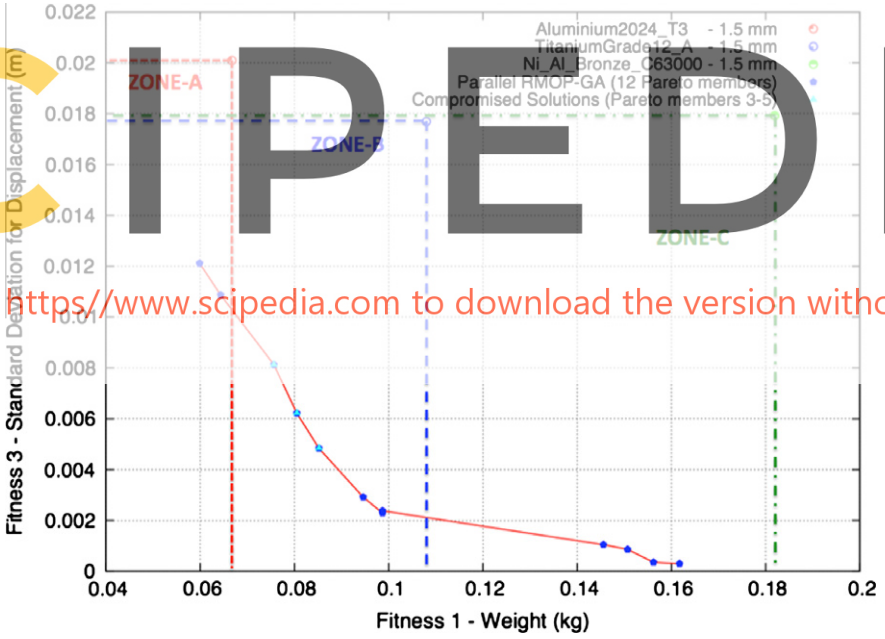

Fig. 10. Fitness 1 (Weight) vs. Fitness 3 (Standard Deviation of Displacement).

Pareto members have lower NMD and SDD when compared to three metal structures with Al-A, Ti-A and Ni-A, except the Pareto member 1 which is only better compared to the metal structure with Al-A. Fig. 12 illustrates 3D view of Pareto distribution. In overall, all Pareto members have lower weight and lower mean displacement with lower sensitivity displacement for all three critical load cases. Three Pareto members 1 (the best solution for the fitness 1), 4 (compromised solution), and 12 (the best solution for fitness functions 2 and 3) are selected for further comparisons.

Table 8 compares the value for three fitness functions obtained by three metal structures, and Pareto members 1, 4, and 12. Pareto members 1, 4 and 12 have better mechanical properties in terms of weight and mean displacement and also they have better robustness (insensitivity or stability) when compared to three metal structures with Al-A, Ti-A and Ni-A at all three critical load cases.

Table 9 shows the stacking sequence of Pareto members 1, 4 and 12. It can be seen that all Pareto members use Al-A at the middle and bottom layers. Table 10 compares the actual displacement obtained for Pareto members 1, 4 and 12 and three metal structures with Al-A, Ti-A and Ni-A. For load cases 1, 2 and 3, Pareto member 1 has lower displacement by 38.6%, 18.4% and 8.0% when compared to the metal structure with Al-A. Pareto member 4 reduces displacement by 63.9% (Case1), 7.1% (Case 2) and 42.7% (Case 3) compared with the metal structure with Ti-A. In the same way Pareto member 12 produces lower displacement for load cases 1, 2 and 3 of -97.9%, -69.4% and -84.4% compared to the metal

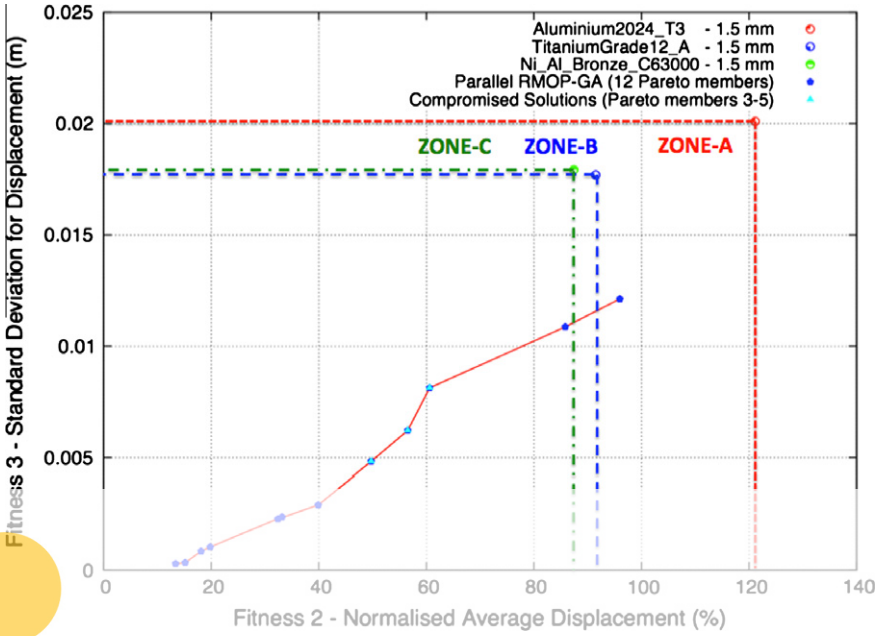

Fig. 11. Fitness 2 (Normalised Average Displacement) vs. Fitness 3 (Standard Deviation of Displacement).

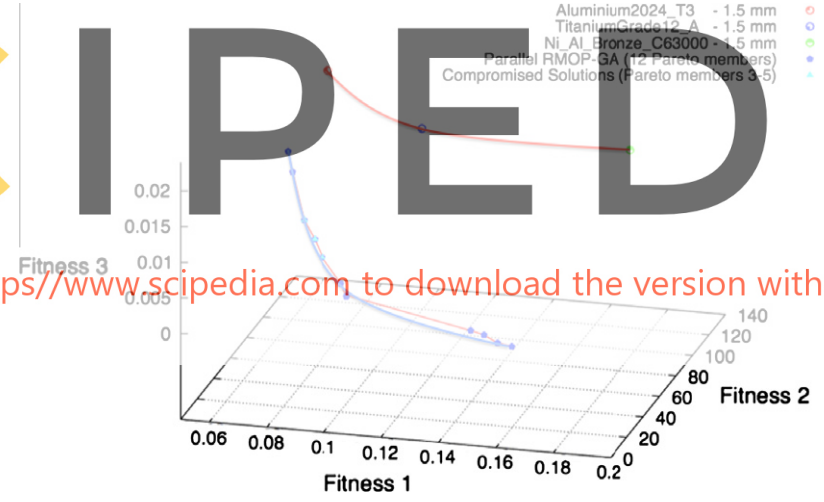

Fig. 12. Pareto front for the three fitness function: fitness 1 (weight), fitness 2 (NMD) and fitness 3 (SDD).

Table 8
Comparison fitness values for weight, normalised mean displacement (NMD) and Standard Deviation Displacement (SDD).

Type of metal/hybrid composite	Weight (kg)	NMD (%)	SDD
Metal structure Al-A	0.067	121.1	0.0201
PM1 (best solution for weight)	0.059 (−10.3%)	95.9 (−20.7%)	0.0121 (−39.8%)
Metal structure Ti-A	0.108	91.5	0.0177
PM4 (compromised solution)	0.080 (−25.4%)	56.5 (−38.2%)	0.0062 (−64.8%)
Metal structure Ni-A	0.182	87.4	0.0180
PM12 (best solution for Stiffness)	0.161 (−11.1%)	13.3 (−84.7%)	0.0002 (−98.4%)

Table 9
Stacking sequence of Pareto member solutions 1, 4 and 12 (*Note*: Thickness and orientation for metal layer i.e. *Mt* = 0.3 mm and *Mo* = 0 not apply for metal).

Pareto member	Stacking sequence (ID)	Thickness (ID)	Orientation angle (ID)
Pareto member 1 (best weight solution)	1311121	*Mt*31*Mt*21*Mt*	*Mo*81*Mo*28*Mo*
Pareto member 4 (compromised solution)	2351211	*Mt*35*Mt*11*Mt*	*Mo*21*Mo*88*Mo*
Pareto member 12 (best stiffness solution)	1221111	*Mt*93*Mt*411 *Mt*	*Mo*83*Mo*18*Mo*

Table 10
Comparison of actual displacement obtained by fiber metal Pareto members 1, 4 and 12, and MS Al-A, MS Ti-A and MS Ni-A (Note: PMi represents the ith Pareto member).

Metal/Pareto member (HCS)	Case 1 (m)	Case 2 (m)	Case 3 (m)
MS Al-A	0.036303	0.00050512	0.0025665
PM1 (best Weight solution)	0.022304 (−38.6%)	0.00041223 (−18.4%)	0.0023622 (−8.0%)
MS Ti-A	0.031680	0.000363	0.001775
PM4 (compromise solution)	0.011439 (−63.9%)	0.000337 (−7.1%)	0.0010162 (−42.7%)
MS Ni-A	0.032046	0.000321	0.001717
PM12 (best stiffness solution)	0.0006738 (−97.9%)	0.000098342 (−69.4%)	0.000268 (−84.4%)

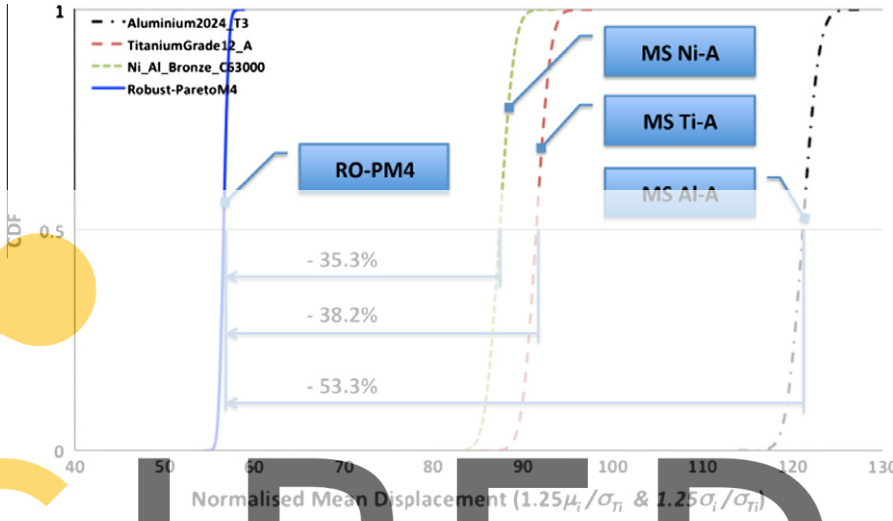

Fig. 13. Comparison of CDF obtained by MS Al-A, MS Ti-A, MS Ni-A and PM4 (*Note*: RO-PM*i* represents the *i*th robust optimal Pareto member).

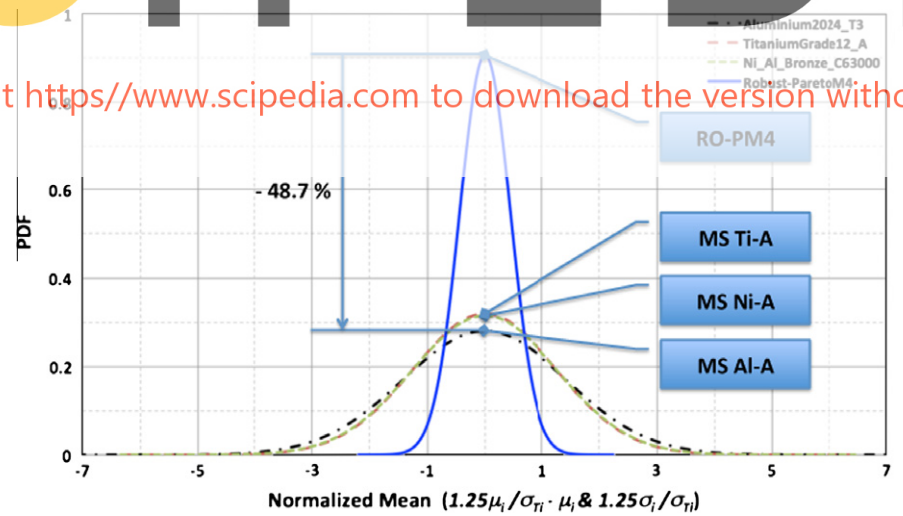

Fig. 14. Comparison of PDF obtained by MS Al-A, MS Ti-A, MS Ni-A and PM4 (*Note*: RO-PM*i* represents the *i*th robust optimal Pareto member).

structure with Ni-A. It can be seen that the optimal HCS has superiority on both mechanical properties and its mechanical behaviours at uncertain critical load cases.

Both the NMD and SDD obtained by metal structures with Al-A (denoted as MS Al-A), Ti-A (denoted as MS Ti-A), Ni-A (denoted as MS Ni-A) and Pareto member 4 (the compromised robust solution: marked as RO-PM4) can be compared using Cumulative Distribution Function (CDF) and Probability Density Function (PDF). Fig. 13 compares the CDF obtained by MS Al-A, MS Ti-A and MS Ni-A, and RO-PM4. It can be seen that RO-PM4 reduces the NMD by 35, 38 and 53% when compared to MS Al-A, MS Ti-A and MS Ni-A. MS Ni-A has lower displacement among three metals. The SDD (sensitivity) can be represented by evaluating gradient of the lines from the CDF value of 0 to value of 0.5 or 1 (steeper gradient = lower sensitivity) however PDF is plotted in Fig. 14 to have a clear sensitivity comparison between MS Al-A, MS Ti-A, MS Ni-A and RO-PM4. It can be seen that the optimal solution RO-PM4 has lower sensitivity (narrower and taller bell curve) when compared to three metal structures. RO-PM4 has approximately 48% lower SDD when compared to all MS Al-A, MS Ti-A and MS Ni-A. MS Ti-A has lower SDD among three MS references. In other words, the robust design method has capabilities to produce a set of

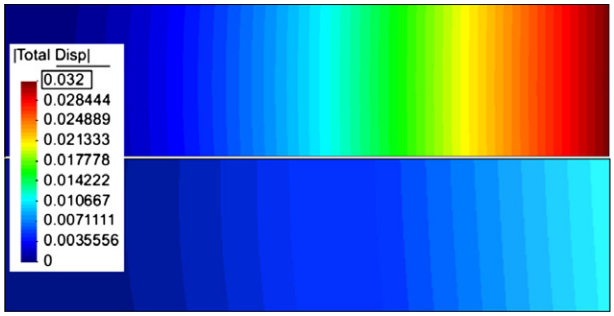

Fig. 15. Comparison of displacement contours for Case 1 obtained by metal structure reference Ti-A (top) and Pareto member 4 (bottom) at a displacement range of [0:0.032 m].

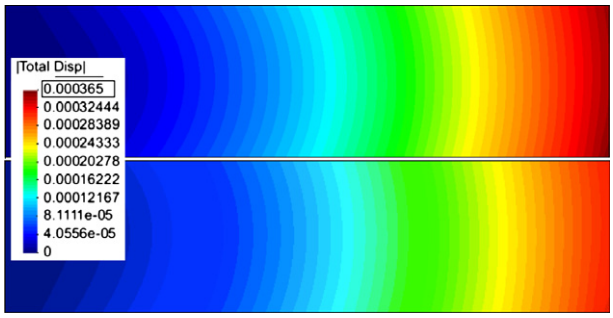

Fig. 16. Comparison of displacement contours for Case 2 obtained by metal structure reference Ti-A (top) and Pareto member 4 (bottom) at a displacement range of [0:0.000365 m].

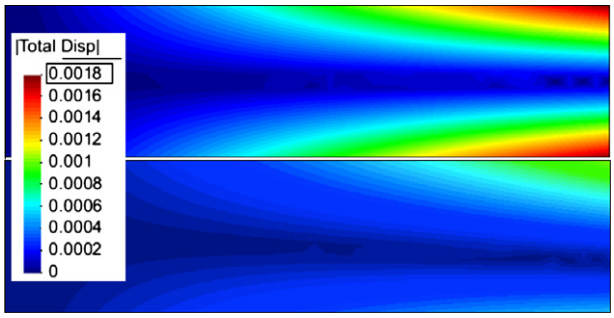

Fig. 17. Comparison of displacement contours for Case 3 obtained by metal structure reference Ti-A (top) and Pareto member 4 (bottom) at a displacement range of [0:0.0018 m].

solutions that have lower displacement and lower sensitivity at the variance of uncertain load cases.

Figs. 15 and 16 compares displacement contours obtained by the reference metal structures with Ti-A and Pareto member 4 (see Fig. 17). It can be seen that Pareto member 4 have lower displacement for three critical load cases.

5. Conclusions

In this paper, a methodology for the Robust Multi-Objective Design Optimisation of advance Hybrid Composite Structures has been developed. The methodology couples a robust multi-objective evolutionary algorithm and a Finite Element Method based composite structure analysis tool under a parallel computing system. It has been implemented to improve the Hybrid Composite Structure in terms of the mechanical properties (weight, and stiffness) and the stability of the mechanical behaviors at the variable critical load cases (bending, shear and torsion). Numerical results demonstrate that the hybrid (fiber metal laminated) composite structures obtained by the robust design offer better mechanical properties and more stable mechanical behavior under uncertain load conditions than currently available metal structures. Analytical research shows that Pareto optimal solutions obtained from the optimisation offers a set of selections to design engineers so that they may proceed into more detail phases of the composite structure design process. Ongoing research focuses on the robust design optimisation of composite structural damping frequency.

References

[1] Vlot A. Impact loading on fibre metal laminates. Int J Impact Eng 1996;18(3):291–307.
[2] Vlot A, Gunnink JW. Fibre metal laminates. Kluwer Academic Publishers; 2001.
[3] Botelho EC, Campos AN, de Barros E, Pardini LC, Rezende MC. Damping behavior of continuos fiber/metal composite materials by the free vibration method. Composites: Part B 2006;37:255–63.
[4] Le Bourlegat LR, Damato CA, da Silva DF, Botelho EC, Pardini LC. Processing and mechanical characterization of titanium–grafite hybrid laminates. J Reinf Plast Compos 2010;29:3392–400.
[5] Caprino G, Spataro G, Del Luongo S. Low-velocity impact behavior of fibreglass-aluminium laminates. Composites: Part A 2004;35:605–16.
[6] Khalili SMR, Mittal RK, GharibiKalibar S. A study of the mechanical properties of steel/aluminium/GRP laminates. Mater Sci Eng A 2005;412:137–40.
[7] Vogelesang LB, Vlot A. Development of fibre metal laminates for advanced aerospace structures. J Mater Process Technol 2000;103:1–5.
[8] Vermeeren CAJR, Beumler Th, deKanter JLCG, vanderJagt OC, Out BCL. GLARE design aspects and philosophies. Appl Compos Mater 2003;10:257–76.
[9] Afaghi-Khatibi A, Lawcock G, Ye L, Mai YW. On the fracture mechanical behaviour of fibre reinforced metal laminates (FRMLs). Comput Meth Appl Mech Eng 2000;185:173–90.
[10] Davidson DL, Austin LK. Fatigue crack growth through ARALL-4 at ambient temperature. Fatigue Fract Eng Mater Struct 1991;14:939–51.
[11] Sinke J. Manufacturing of GLARE parts and structures. Appl Compos Mater 2003;10:293–305.
[12] Kawai M, Morishita M, Tomura S, Takumida K. Inelastic behaviour and strength of fibermetal hybrid composite: GLARE. Int J Mech Sci 1998;40:183–98.
[13] Nam HW, Hwang W, Han KS. Stacking sequence design of fiber–metal laminate for maximum strength. J Compos Mater 2001;35:1654–83.
[14] Peng W, Chen J, Wei J, Tu W. Optimal strength design for fibermetal laminates and fiber-reinforced plastic laminates. J Compos Mater 2011;45:237–54.
[15] Taguchi G. Introduction to quality engineering: designing quality into products and processes. Qual Res 1986.
[16] Lee DS, Periaux J, Gonzalez LF, Srinivas K, Onate E. Robust multidisciplinary unmanned aerial system design optimisation. Int J Struct Multidisciplinary Optimiz; 2011. p. 1–18, doi: 10.1007/s00158-011-0705-0.
[17] Lee DS, Gonzalez LF, Srinivas K, Periaux J. Robust design optimisation using multi-objective evolutionary algorithms. Special Issue: An Int Comput Fluid 2008;37(5):565–83.
[18] Walker M, Hamilton R. A technique for optimally designing fibre-reinforced laminated plates with manufacturing uncertainties for maximum buckling strength. Eng Optim 2005;37:135–44.
[19] Adali S, Lene F, Duvaut G, Chiaruttini V. Optimization of laminated composites subject to uncertain buckling loads. Compos Struct 2003;62:261–9.
[20] Liao Y, Chiou CY. Robust optimum designs of fiber-reinforced composites using constraints with sensitivity. J Compos Mater 2006;40:2067–81.
[21] António CC, Hoffbauer LN. An approach for reliability-based robust design optimisation of angle-ply composites. Compos Struct 2009;90:53–9.
[22] Lee MCW, Mikulik Z, Kelly DW, Thomson RS, Degenhardt R. Robust design – a concept for imperfection insensitive composite structures. Compos Struct 2010;92:1469–77.
[23] Lee DS, Gonzalez LF, Periaux J, Bugeda G. Double shock control bump design optimisation using hybridised evolutionary algorithms. Special Issue Evolut Comput Aeros Sci – J Aeros Eng 2011;225(10):1175–92.
[24] Lee DS, Morillo C, Bugeda G, Oller S, Onate E. Multilayered composite structure design optimisation using distributed/parallel multi-objective evolutionary algorithms. J Compos Struct 2012;94(3):1087–96.
[25] Oller S. Simulación numérica del comportamiento mecánico de los materiales compuestos, CIMNE; 2003.
[26] Deb K. Multi-objective optimisation using evolutionary algorithms. Wiley; 2003.
[27] Deb K, Agrawal S, Pratap A, Meyarivan T. A fast and elitist multi-objective genetic algorithm: NSGA-II. IEEE Trans Evolut Comput 2002;6(2):182–97.
[28] Gen M, Cheng R. Genetic algorithm and engineering design. 1st ed., John Wiley and Sons Inc.; 1997.
[29] Kenndedy J, Eberhart R. Particle swarm optimization. Proc IEEE Int Conf Neural Network 1995;IV:1942–8.

[30] Rastellini F, Oller S, Salomón O, Oñate E. Composite material non-linear modelling for long fibre-reinforced laminates. Continuum basis, computational aspects and validations. Comput Struct 2008;86:879–96.
[31] Car E, Oller S, Oñate E. A large strain plasticity for anisotropic materials: composite material application. Int J Plast 2001;17(11):1437–63.
[32] Martinez X, Rastellini F, Flores F, Oller S, Oñate E. Computationally optimized formulation for the simulation of composite materials and delamination failures. Composites: Part B 2011;42(2):134–44.
[33] Soden PD, Hintonb MJ, Kaddoura AS. Lamina properties, lay-up configurations and loading conditions for a range of fibre-reinforced composite laminates. Compos Sci Technol 1998;58:1011–22.
[34] Department of Defence of USA. Composite Materials Handbook, Polymer Matrix Composites Materials Usage, Design, and, Analysis, MIL-HDBK-17/3F, vol. 3; 2002.
[35] Online Materials Information Resource. <http://www.matweb.com/index.aspx.com>.